# EFFECT OF PRINCIPAL STRESS ROTATION ON SHEAR MODULUS $G_{max}$ OF GAP-GRADED SOIL SUBJECTED TO INTERNAL EROSION

The University of Tokyo Student Member ○Sanjei Chitravel
The University of Tokyo Regular Member Masahide Otsubo
The University of Tokyo Fellow Member Reiko Kuwano

## 1. INTRODUCTION

Internal erosion is the transportation of soil particles from within or beneath a water-retaining structure due to the seepage flow, impacting the mechanical and hydraulic behaviour of soil. The result of internal erosion can be observed in the field as chains of macropores on the ground surface. The degree of migration of fine particles can affect both micro and macro structural behaviours of soil. Many researchers have conducted experimental investigations on different aspects of internal erosion such as the susceptibility of soil and progression of internal erosion using gap-graded soils. However, a few studies have tried to explore the post-erosion shear modulus with a distinct internal fabric. This paper analyses the impacts of internal erosion on the variation in small strain shear modulus of eroded soil under different principal stress directions.

## 2. MATERIAL PROPERTIES

Silica sand No. 5 ($D_{50}$=530 µm) and silica powder ($d_{50}$ = 17 µm) were used as coarse and fine materials, respectively, having the same specific gravity ($G_s$) of 2.645. According to the Unified Soil Classification System (USCS), fines are the particles passing the 75 µm sieve, and thus silica powder was selected as a non-plastic fine in this study. They were produced at the same mining site where fragments crushed from rocks were sieved into different sizes. Thus, their mineralogy was assumed to be almost identical. In this study, a fines content ($FC$) of 20% was selected to make the gap-graded soil (silica mixture) following similar approaches by the prior studies. The tested gap-graded soil is internally unstable, and the fine particles could be washed out during erosion.

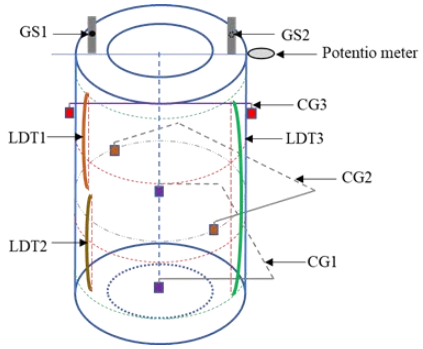


**Fig. 1** Set up of transducers used in HCTA

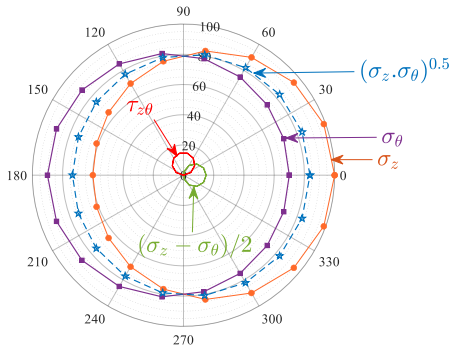


**Fig. 2** Typical stress path of PSR in HCTA

## 3. TEST METHOD

A hollow cylindrical torsional shear test apparatus (HCTA) was employed in this study. The tested specimens had outer diameter $D_o$=100 mm, inner diameter $D_i$=60 mm and height H=100 mm. All transducers used are shown in Fig. 1. An external displacement transducer (EDT) was placed outside the cell to measure the axial strain ($\varepsilon_a$) of the specimen. The local axial strain ($\varepsilon_a^{LDT}$) and radial strain ($\varepsilon_r$) were calculated from the local displacement transducers (LDTs) and clip gauges (CGs). A potentiometer was used to measure a large torsional shear strain ($\gamma_{z\theta}$), which was attached to the loading shaft outside the cell. A pair of gap sensors (GS1 and GS2) embedded on the top platen in the cell were used to measure small-range torsional shear strain ($\gamma_{z\theta}^{GS}$) between 0.001% and 2%. Following the specimen preparation using the moist tamping method (Ladd, 1978), 30 kPa of isotropic confining pressure was imposed on the specimen and maintained until the end of the test. Then double vacuum and saturation were applied to reach B>0.95. After applying 200 kPa backpressure (230 kPa cell pressure), the specimen was consolidated to an effective stress of 80 kPa. After that soil specimen was eroded using back pressure (<10 kPa) applied through the water tank. A turbidity meter was used to measure the turbidity of the collected water every 1hr for 20 hrs. Finally, as shown in Fig. 2, the rotation of the major principal stress was started by controlling $\sigma_z$ (vertical), $\sigma_\theta$ (circumferential) and $\tau_{z\theta}$ (shear) to apply a constant deviator stress $\sqrt{{\tau_{z\theta}}^2 + [(\sigma_z - \sigma_\theta)^2/4]}$ while increasing the direction of the major principal stress from the vertical direction $2\alpha$ $[\tan^{-1}(2\tau_{z\theta}/(\sigma_z - \sigma_\theta))]$ from 0° to 360°, while keeping the mean effective stress 80 kPa as constant. Further small torsional cyclic loadings were applied at each interval of 10° under drained conditions, where samples with relative densities, $D_{r0}$ of 80% (dense), 50% (medium dense) and 30% (loose) were subjected to seepage or not (intact) prior to the application of cyclic loadings.

Keywords: Gap-graded soil, Internal erosion, Principal stress rotation, Drained
Contact address: Institute of Industrial Science, 4-6-1, Komaba, Meguro, Tokyo 153-8505, Japan, Tel: 03-5452-6843

## 4. RESULTS AND DISCUSSIONS

Fig. 3 illustrates the relationship between $\tau_{z\theta}$ and $\gamma_{z\theta}$ during the full rotation of principal stress axes under stress ratio $R_1$ ($\sigma_1'/\sigma_3'$) of 1.43. It is obvious that induced $\gamma_{z\theta}$ and breadth of the hysteresis loop are higher for the eroded specimen. However, a lower $\varepsilon_a$ is observed for the eroded specimen after one full rotation. From the overall perspective, it is worth noting that, by defining the gradient of the line through the extreme points on the whole loop as a secant shear modulus, the non-eroded (*NE*) specimen showed a larger value than the eroded (*E*) specimen.

Cyclic torsional loading at small-strain levels ($\gamma$ < 0.001%) was applied at an interval of 10° in order to estimate the small strain shear modulus, $G_{max}$ of specimen. At 0°, post-erosion $G_{max}$ increases compared with *NE* $G_{max}$ under the same stress amplitude. This could be due to the force chains benefiting from an increase in inter-particle contacts caused by the rearrangement of the soil skeleton during erosion at the low strain range. Fig. 4 shows the influence of rotating principal stress direction on $G_{max}$ of *NE* and *E* specimens. It indicates that $G_{max}$ increases firstly and exhibits a tendency for degradation followed by a growth with increasing $\alpha$. However, at the end of rotation $G_{max}$ is lower than the initial $G_{max}$. Thus, the obtained results indicate that the shear stress direction is dependent on the shear modulus under the same magnitude of normal stresses, which could be due to shape of coarse particles and distribution of fines. Further, the overall trend of $G_{max}$ of *NE* and *E* specimens are quite similar in the pattern. It seems within -20°<$\alpha$<220°, eroded specimens show higher $G_{max}$, which could be attributed to the seepage direction and temporary force chains. Moreover, the reinforced soil skeleton established by the erosion did not resist against shear loading.

The relationships between the normalized shear modulus ($G_{2\alpha}^*/G_0^*$) and $\alpha$ are shown in Fig. 5. $G_{2\alpha}^*/G_0^*$ is given by:

$$G_{2\alpha}^*/G_0^* = \frac{G_{2\alpha}/f(e_{2\alpha})}{G_0/f(e_0)} \text{, where } f(e) = \frac{(2.17-e)^2}{(1+e)}$$

It is seen that after normalisation, a highly non-linear response of the shear modulus was observed, which is proportional to $\tau_{z\theta}$ values. In cases of *NE* and *E*, the max and min values for the normalised shear modulus were found at $\alpha$ of 70° and 130°, which are density dependent. In addition, such trends in behavior might also be attributed to the effects of the various anisotropic stress states, which possibly induced slight changes to the initial fabric. The distribution of fine particles and anisotropy induced by seepage flow contribute to an unpredictable mechanical behaviour of gap-graded soil.

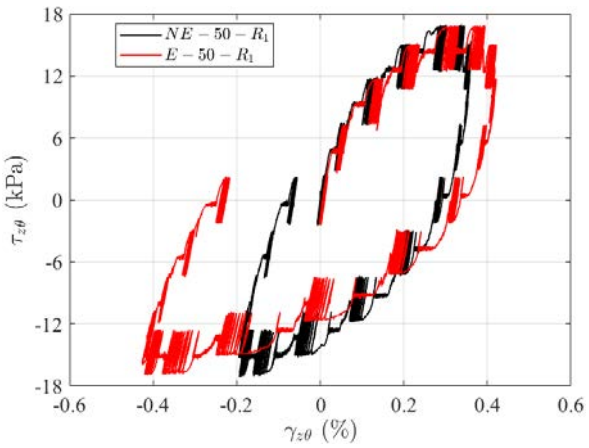


**Fig. 3** Variation in shear strain ($\gamma_{z\theta}$) with shear stress ($\tau_{z\theta}$) during principal stress rotation (PSR)

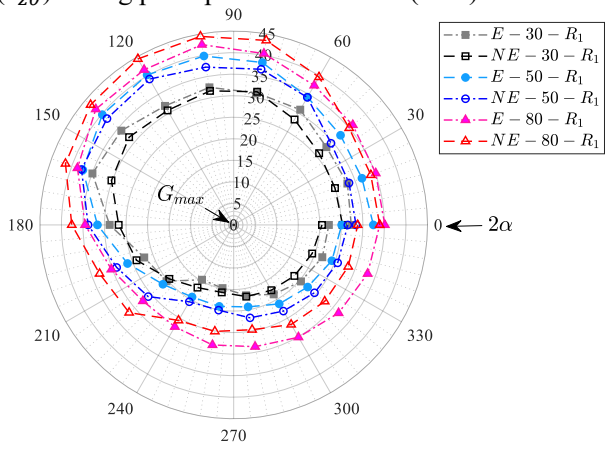


**Fig. 4** Variation of $G_{max}$ major principal direction $2\alpha$

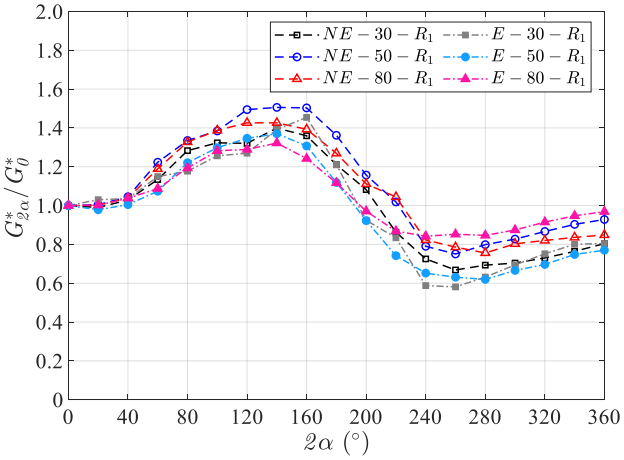


**Fig. 5** Variation of normalised small-strain shear modulus ($G_{2\alpha}^*/G_0^*$) with major principal direction $2\alpha$

## 5. CONCLUSION

An experimental investigation was conducted to study the post-erosion shear modulus of gap-graded soil under principal stress rotation (PSR). After a whole cycle, induced post-erosion $\gamma_{z\theta}$ is increased while $\varepsilon_a$ is decreased due to seepage flow accompanied with fine removal. In PSR, the specimens subjected to erosion exhibit a reduction in $G_{max}$ compared to *NE* specimens with increasing $\alpha$. The reduction of the $G_{max}$ might be due to the inefficacy of the reinforced soil skeleton established by the erosion against shear loading.

## REFERENCES

Ladd, R.S.: Preparing test specimens using under compaction, Geotechnical Testing Journal, 1-1, 1978, pp.16-23.
Yang, Y., Kuwano, R.: Effects of principal stress rotation on small strain stiffness of sand subjected to piping erosion, Soils and Foundations, 57-5, 2017, pp.776-788.